One-neutron knockout in the vicinity of the $N = 32$ sub-shell closure: ^{9}Be(^{57}Cr,^{56}Cr+γ)X

A. Gade,[1,2] R. V. F. Janssens,[3] D. Bazin,[1] B. A. Brown,[1,2] C. M. Campbell,[1,2] M. P. Carpenter,[3] J. M. Cook,[1,2] A. N. Deacon,[4] D.-C. Dinca,[1,2] S. J. Freeman,[4] T. Glasmacher,[1,2] M. Horoi,[5] B. P. Kay,[4] P. F. Mantica,[1,6] W. F. Mueller,[1] J. R. Terry,[1,2] J. A. Tostevin,[7] and S. Zhu[3]

[1]*National Superconducting Cyclotron Laboratory, Michigan State University, East Lansing, Michigan 48824, USA*
[2]*Department of Physics and Astronomy, Michigan State University, East Lansing, Michigan 48824, USA*
[3]*Physics Division, Argonne National Laboratory, Argonne, Illinois 60439, USA*
[4]*School of Physics and Astronomy, Schuster Laboratory, University of Manchester, Manchester M13 9PL, United Kingdom*
[5]*Department of Physics, Central Michigan University, Mount Pleasant, Michigan 48859, USA*
[6]*Department of Chemistry, Michigan State University, East Lansing, Michigan 48824, USA*
[7]*Department of Physics, School of Electronics and Physical Sciences, University of Surrey, Guildford, Surrey GU2 7XH, United Kingdom*

(Received 22 May 2006; published 11 October 2006)

The one-neutron knockout reaction ^{9}Be(^{57}Cr,^{56}Cr+γ)X has been measured in inverse kinematics with an intermediate-energy beam. Cross sections to individual states in ^{56}Cr were partially untangled through the detection of the characteristic γ-ray transitions in coincidence with the reaction residues. The experimental inclusive longitudinal momentum distribution and the yields to individual states are compared to calculations that combine spectroscopic factors from the full *fp* shell model and nucleon-removal cross sections computed in a few-body eikonal approach.

DOI: 10.1103/PhysRevC.74.047302 PACS number(s): 24.50.+g, 21.10.Jx, 25.60.Gc, 27.40.+z

Neutron-rich Ca, Ti, and Cr isotopes have attracted much attention recently. The strong proton-neutron monopole interaction in these exotic nuclei with $\pi f_{7/2}\nu(fp)$ configurations causes a shift in the energy of the $\nu f_{5/2}$ neutron single-particle orbit as protons fill the $\pi f_{7/2}$ shell and results in the development of an $N = 32$ sub-shell closure in ^{52}Ca, ^{54}Ti, and ^{56}Cr [1]. Nuclei in the vicinity of this new sub-shell closure have been studied extensively in β-decay experiments [2–5], intermediate-energy Coulomb excitation [6,7], deep-inelastic heavy-ion collisions [8,9], fusion-evaporation reactions [10–12], and secondary fragmentation [13].

We report on the study of the one-neutron knockout reaction ^{9}Be(^{57}Cr,^{56}Cr+γ)X. Direct one-nucleon removal at intermediate beam energies [14] has been used extensively to study single-particle structure in neutron-rich and proton-rich exotic nuclear species (see, e.g., Refs. [15–20]). Single-particle cross sections and longitudinal momentum distributions are computed using few-body reaction theory, in the eikonal and sudden approximations [21,22], and employing Skyrme–Hartree-Fock calculations [23,24] to reduce uncertainties in the input to the reaction calculation. Spectroscopic factors, which relate to the occupancy of single-particle orbits, can be deduced from experimental cross sections by comparison with reaction theory and pose stringent tests for modern shell-model calculations far from stability [25]. The longitudinal momentum distribution of the knockout residues is used—similar to the angular distribution in low-energy transfer reactions—to identify the orbital angular momentum l carried by the knocked-out nucleon.

In this paper, we discuss the magnitude of the inclusive cross section, the small branch for the knockout to the ground state of ^{56}Cr, and the shape of the inclusive momentum distribution as compared with that predicted on the basis of single-particle strengths from large-scale shell-model calculations in the *fp* shell.

A secondary beam cocktail containing ^{57}Cr was obtained via fast fragmentation of a 130 MeV/nucleon ^{76}Ge primary beam delivered by the Coupled Cyclotron Facility of the National Superconducting Cyclotron Laboratory at Michigan State University. The production target, 423 mg/cm^2 thick ^{9}Be, was located at the mid-acceptance position of the A1900 fragment separator [26]. The separator was operated at 1% momentum acceptance.

The ^{57}Cr projectiles, with an average mid-target energy of 77 MeV/nucleon, interacted with a 375 mg/cm^2 thick ^{9}Be target placed at the pivot point of the large-acceptance, high-resolution S800 magnetic spectrograph [27]. The event-by-event particle identification and reconstruction of the momentum distribution of the knockout residues were performed with the focal-plane detector system [28]. The energy loss in the S800 ionization chamber, time of flight (TOF) taken between plastic scintillators, and position and angle information of the reaction products in the S800 focal plane were employed to identify the reaction residues produced upon collision with the ^{9}Be target (Fig. 1). The spectrograph was operated in focus mode, where the incoming exotic beam is momentum focused onto the secondary reaction target. The difference in the TOF measured between two scintillators before the secondary target provided the particle identification of the incoming beam. Selection of the incoming species allowed a separation of knockout residues and fragmentation products of the different constituents of the beam. Incoming ^{55}V and ^{57}Cr projectiles overlapped in TOF, but possible contamination from ^{56}Cr produced by proton pickup on ^{55}V was highly unlikely because of momentum mismatch.

An inclusive cross section of $\sigma_{\rm inc} = 122(8)$ mb was determined for the one-neutron knockout from ^{57}Cr to all

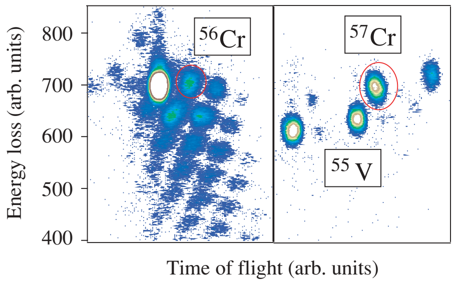

FIG. 1. (Color online) Energy loss vs TOF particle identification spectra for the one-neutron knockout reaction setting and the unreacted incoming beam. Right: incoming, unreacted cocktail beam passing through the ^{9}Be target. This unreacted setting was used to determine normalization of the incoming rate of ^{57}Cr. Left: spectrum obtained with the one-neutron removal reaction residues centered in the S800 focal plane. A software gate was applied on incoming ^{55}V and ^{57}Cr in the TOF difference measured between two plastic scintillators before the target.

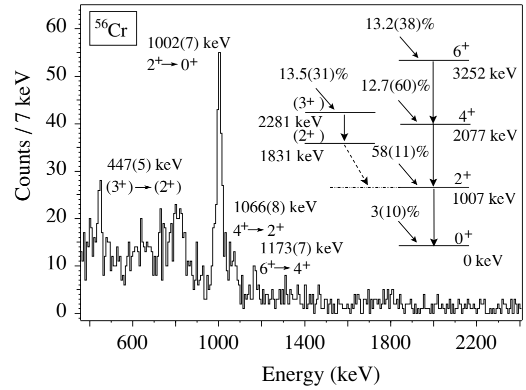

FIG. 2. γ-ray spectrum detected in coincidence with ^{56}Cr knockout residues. Observed transitions agree with the level scheme established in [10,11]. Population of individual excited states in the knockout reaction is derived from γ-ray intensities relative to the number of knockout residues, taking the level scheme into account. The fraction of 2.6% for the knockout to the ground state is obtained after subtraction.

bound final states of ^{56}Cr. This was obtained from the yield of knockout residues divided by the number of incoming projectiles relative to the number density of the ^{9}Be target. The fraction of incoming ^{57}Cr projectiles in the cocktail was determined from the unreacted spectrograph setting shown in the right panel of Fig. 1. The number of incoming ^{57}Cr in the reaction setting is then derived from this fraction relative to scalers counting the total incoming particle flux. The main uncertainties stem from the choice of the software gates used for particle identification (2.5%), beam composition (3%), and momentum acceptance of the S800 spectrograph (5%). These systematic errors are assumed to be independent and have been added in quadrature.

The ^{9}Be reaction target was surrounded by an array of 32-fold segmented high-purity Ge detectors (SeGA) [29], arranged in a configuration with two rings (90° and 37° central angles with respect to the beam axis, equipped with ten and seven detectors, respectively). The segmentation of the detectors allows an event-by-event Doppler reconstruction that deduces the angle of the γ-ray emission from the position of the segment that registered the highest energy deposition.

The SeGA total photopeak efficiency of 2.2% for the 1.33 MeV photon energy was determined with standard calibration sources. Those sources also provided the detector response used to correct the in-beam data for the Lorentz boost arising from the velocity of the emitting reaction residues ($v/c = 0.36$).

The Doppler-reconstructed γ-ray spectrum detected in coincidence with ^{56}Cr reaction residues is shown in Fig. 2. The γ-ray transitions observed in the present experiment agree with the results from [10,11] and confirm the known level scheme, given as an inset in Fig. 2. Using the known γ-ray branching ratios and the level scheme, the cross sections for the one-neutron knockout to specific final states were deduced from the balance between the observed feeding and deexcitation patterns. These intensity balances can be rather uncertain in instances where unobserved γ-ray decays are possible.

The spectroscopic factors leading to the ground state and the 2^+ state (1.007 MeV) of ^{56}Cr were calculated in the full *fp* shell-model space with the GXPF1A interaction [30,31] using the codes CMICHSM [32] and OXBASH [33]. The results are summarized in Fig. 3 and Table I. The calculations predict a $3/2^-$ ground state for ^{57}Cr, which agrees with an early β-decay measurement [34] and is consistent with more recent experimental observations [3,12]. The calculations indicate a severely fragmented single-particle strength as the derived spectroscopic factors are $C^2S(0^+, p_{3/2}) = 0.24$, $C^2S(2^+, p_{3/2}) = 0.32$, $C^2S(2^+, f_{7/2}) = 0.03$, $C^2S(2^+, f_{5/2}) = 0.006$, and $C^2S(2^+, p_{1/2}) = 0.007$, with the remaining spectroscopic strength, which sums up to the neutron occupation number of 13, going to levels up to about 8 MeV in ^{56}Cr (the neutron decay threshold is $S_n = 8.26$ MeV [35]). Such high excitation energies imply that there may be several hundred levels to consider. For an estimate of the cross section related to these states, we take the remaining ($p_{1/2}$, $f_{5/2}$, $p_{3/2}$) strength of $C^2S(p_{3/2}) = 2.15$, $C^2S(f_{5/2}) = 1.81$, and $C^2S(p_{1/2}) = 0.47$

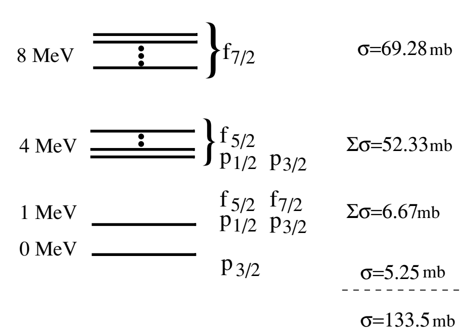

FIG. 3. Schematic shell-model level scheme, configurations, and resulting theoretical cross sections for the population of excited states in ^{56}Cr. The shell-model calculation is schematic. Cross sections are calculated from eikonal reaction theory as described in the text (Table I).

TABLE I. Results of the schematic calculation of the knockout process from ^{57}Cr to ^{56}Cr. Energy E_f of the final state in ^{56}Cr, spectroscopic factor C^2S for the neutron knockout from orbit *nlj*, stripping and diffractive contributions to σ_{sp}, and resulting theoretical partial cross section σ_i as calculated in the few-body eikonal reaction theory.

E_f (MeV)		*nlj*	C^2S	σ_{str} (mb)	σ_{dif} (mb)	σ_{sp} (mb)	σ_i (mb)
0.0	0_1^+	$2p_{3/2}$	0.24	14.56	6.17	20.73	5.25
1.0	2_1^+	$2p_{3/2}$	0.32	12.83	5.15	17.98	6.07
		$1f_{7/2}$	0.03	9.57	3.18	12.75	0.40
		$1f_{5/2}$	0.006	8.07	2.61	10.67	0.07
		$2p_{1/2}$	0.007	12.87	5.17	18.04	0.13
4.0		$2p_{3/2}$	2.15	9.57	3.37	12.94	29.33
		$1f_{5/2}$	1.81	6.70	1.97	8.67	16.55
		$2p_{1/2}$	0.47	9.63	3.40	13.02	6.45
8.0		$1f_{7/2}$	7.97	6.47	1.78	8.24	69.28
		Sum	13			Sum	133.5

to be centered at 4 MeV in excitation and the deeper $f_{7/2}$ hole strength of about 8 units to be centered at 8 MeV in excitation energy. Clearly, the value $C^2S(f_{7/2}) = 8$ should be viewed as an upper limit for $f_{7/2}$ occupation as it assumes that no spectroscopic strength is lost to unbound states above the neutron threshold. This complex scenario with spectroscopic strength to many excited states below threshold leads to the following conclusion: the measured population of excited states quoted in Fig. 2 must include both the direct population in the one-neutron knockout process and unobserved, discrete feeding from many higher-lying excited states. The high partial cross section carried by the 2_1^+ state is likely dominated by indirect, unobserved feeding. This state will act as a doorway state funneling most of the spectroscopic strength feeding the higher-lying, excited states that are predicted to be populated in the one-neutron knockout by the shell-model calculation.

The theoretical cross sections quoted in Fig. 3 are obtained by combining the spectroscopic factors from the shell-model calculations and the single-particle cross sections from eikonal reaction theory in the following way: the cross sections $\sigma_i(I^\pi)$ for the knockout of a single nucleon with quantum numbers (n, l, j), leaving the core in a specific final state I^π, factorize into a part that describes nuclear structure (the spectroscopic factor C^2S) and a contribution characterizing the reaction process (the single-nucleon removal unit cross section σ_{sp}) as

$$\sigma_i(I^\pi) = \sum_j \left(\frac{A}{A-1}\right)^3 C^2S(j, I^\pi)\sigma_{sp}(j, S_n + E_f(I^\pi)), \quad (1)$$

with summation over all the allowed angular-momentum transfers j. The A-dependent term is a center-of-mass correction [36,37] to the shell-model spectroscopic factors in the *fp* shell. The effective separation energy of the nucleon is $S_n + E_f(I^\pi)$, where $S_n = 5.176$ MeV is the ground-state neutron separation energy of the projectile [35] and $E_f(I^\pi)$ denotes the excitation energy of the final state of the core. The single-particle cross sections are the sum of contributions from both the stripping and diffractive dissociation mechanisms [14]:

$$\sigma_{sp} = \sigma_{str} + \sigma_{dif}. \quad (2)$$

The σ_{sp} entering Eq. (1) were obtained within the eikonal approach of [14,38]. The σ_{str} and σ_{dif} contributions were computed from the core- and neutron-target S matrices, which were calculated from the ^{9}Be and ^{56}Cr densities using Glauber theory, as discussed in [14]. We assumed a Gaussian matter density for ^{9}Be with a rms radius of 2.36 fm. The ^{56}Cr density was taken from (SKX) Hartree-Fock (HF) calculations [23]. The core-neutron relative motion wave functions were calculated in a Woods-Saxon potential. The diffuseness parameter was fixed at $a = 0.7$ fm, consistent with previous work [14]. The radius parameter r_0 was selected for each single-particle orbit (*nlj*) individually to reproduce the rms separation of neutron and core as calculated within the SKX HF wave function. The depths of the binding potentials were chosen to reproduce the effective separation energy of each final state.

The large inclusive cross section for knockout from ^{57}Cr to ^{56}Cr can be traced to the large neutron occupancy of orbitals that, in one-neutron removal, populate bound excited states of ^{56}Cr. Remarkably, the small theoretical cross section for the knockout to the ground state also agrees with the experimental observation (see Fig. 2) and is a consequence of the very small associated spectroscopic factor of $C^2S = 0.24$. In the shell model, the $2p_{3/2}$, $1f_{5/2}$, and $2p_{1/2}$ single-particle orbits are very close in energy, with the result that a simple description of ^{57}Cr as a single neutron outside a $N = 32$ core fails.

The inclusive parallel momentum distribution of the ^{56}Cr residues is compared with the theoretical expectation in Fig. 4. The latter combines the momentum distributions for the removal of a neutron from $2p_{3/2}$, $1f_{5/2}$, $2p_{1/2}$, and $1f_{7/2}$ orbits (Table I), calculated from the same S matrices as used for the single-particle cross sections, and the method of [22,39]. The theoretical inclusive momentum distribution is then the sum of these individual distributions, weighted with the corresponding spectroscopic factors. The calculated shape

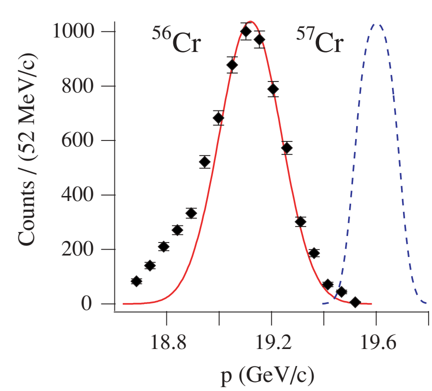

FIG. 4. (Color online) Inclusive parallel momentum distribution of the ^{56}Cr knockout residues compared with theoretical results (solid red line) calculated using the eikonal stripping reaction mechanism. Weights attributed to knockout contributions from $2p_{3/2}$, $1f_{5/2}$, $2p_{1/2}$, and $1f_{7/2}$ orbits were taken from the corresponding theoretical cross sections (Table I). The dashed blue line is the momentum profile of the unreacted ^{57}Cr projectile beam passing through the target.

was convoluted with the measured momentum profile of the unreacted ^{57}Cr beam to account for the incoming momentum spread and the straggling in the target. The measured momentum distribution is asymmetric with the high-momentum side being accurately reproduced by the calculation, while a tail extends toward lower momenta. Such asymmetric shapes have been reported before [40–42] in nucleon knockout reactions of well-bound systems and indicate (as yet unquantified) effects that go beyond eikonal reaction theory. In the eikonal theory, the partial cross sections are determined (i) structurally, by the single-particle overlap for each transition, and (ii) dynamically, by the nucleon- and residue-target S matrices. The expressions for the single-particle cross sections are inclusive with respect to all final states of the target (using completeness) when assuming these can be considered degenerate with the target ground state for the purpose of the reaction dynamics (the adiabatic approximation); the result is that the S matrices are calculated at fixed energy. This is expected to be a very good approximation at intermediate energy. Expressing the eikonal residue momentum distribution requires additional approximations, e.g., the neglect of residue final-state interactions, while this observable now probes the dynamics more closely. This extra sensitivity indicates a small redistribution of the integrated single-particle cross section with momentum compared to that from the approximate (energy nonconserving) eikonal model kinematics, with a low-energy tail characteristic of (dissipative) target excitations that are treated only approximately (adiabatically) in the eikonal model. The approximations required for the integrated partial cross section on the other hand are more robust, as discussed above and in [42]. The overall agreement in the shapes of the measured and calculated inclusive momentum distributions is consistent with the adopted schematic distribution of single-particle strength, and the shell-model space chosen within this approach appears valid.

In summary, this investigation of the one-neutron knockout reaction ^{9}Be(^{57}Cr,^{56}Cr+γ)X has found the spectroscopic strength to be spread over a large number of ^{56}Cr levels. Nevertheless, calculations were able to reproduce the main observables, i.e, the magnitude of the inclusive cross section of $\sigma_{\rm inc} = 122(8)$ mb and the shape of the inclusive parallel momentum distribution. These results further illustrate the potential of direct one-nucleon removal reactions at intermediate energy and the associated theoretical framework for spectroscopic investigations of exotic nuclei.

This work was supported by the National Science Foundation under Grant Nos. PHY-0110253, PHY-9875122, and PHY-0244453, by the U.S. Department of Energy, Office of Nuclear Physics, under Contract No. W31-109-ENG-38, and by the U.K. Engineering and Physical Sciences Research Council Grant No. EP/D003628.

[1] T. Otsuka *et al*., Phys. Rev. Lett. **87**, 082502 (2001).
[2] J. I. Prisciandaro *et al*., Phys. Lett. **B510**, 17 (2001).
[3] P. F. Mantica *et al*., Phys. Rev. C **67**, 014311 (2003).
[4] P. F. Mantica *et al*., Phys. Rev. C **68**, 044311 (2003).
[5] S. N. Liddick *et al*., Phys. Rev. Lett. **92**, 072502 (2004); Phys. Rev. C **70**, 064303 (2004); **72**, 054321 (2005).
[6] D.-C. Dinca *et al*., Phys. Rev. C **71**, 041302(R) (2005).
[7] A. Bürger *et al*., Phys. Lett. **B622**, 29 (2005).
[8] R. V. F. Janssens *et al*., Phys. Lett. **B546**, 55 (2002).
[9] B. Fornal *et al*., Phys. Rev. C **70**, 064304 (2004); **72**, 044315 (2005).
[10] S. Zhu *et al*., Phys. Rev. C, submitted for publication.
[11] D. E. Appelbe *et al*., Phys. Rev. C **67**, 034309 (2003).
[12] A. N. Deacon *et al*., Phys. Lett. **B622**, 151 (2005).
[13] A. Gade *et al*., Phys. Rev. C **73**, 037309 (2006).
[14] P. G. Hansen and J. A. Tostevin, Annu. Rev. Nucl. Part. Sci. **53**, 219 (2003).
[15] A. Navin *et al*., Phys. Rev. Lett. **81**, 5089 (1998).
[16] T. Aumann *et al*., Phys. Rev. Lett. **84**, 35 (2000).
[17] E. Sauvan *et al*., Phys. Lett. **B491**, 1 (2000).
[18] A. Gade *et al*., Phys. Rev. Lett. **93**, 042501 (2004).
[19] J. R. Terry *et al*., Phys. Rev. C **69**, 054306 (2004).
[20] B. A. Brown, P. G. Hansen, B. M. Sherrill, and J. A. Tostevin, Phys. Rev. C **65**, 061601(R) (2002).
[21] J. A. Tostevin, J. Phys. G **25**, 735 (1999).
[22] C. A. Bertulani and A. Gade, Comp. Phys. Comm., **175** 372 (2006).
[23] B. A. Brown, Phys. Rev. C **58**, 220 (1998).
[24] B. A. Brown, W. A. Richter, and R. Lindsay, Phys. Lett. **B483**, 49 (2000).
[25] B. A. Brown, Prog. Part. Nucl. Phys. **47**, 517 (2001).
[26] D. J. Morrissey *et al*., Nucl. Instrum. Methods Phys. Res. B **204**, 90 (2003).
[27] D. Bazin *et al*., Nucl. Instrum. Methods Phys. Res. B **204**, 629 (2003).
[28] J. Yurkon *et al*., Nucl. Instrum. Methods Phys. Res. A **422**, 291 (1999).
[29] W. F. Mueller *et al*., Nucl. Instrum. Methods A **466**, 492 (2001).
[30] M. Honma, T. Otsuka, B. A. Brown, and T. Mizusaki, Phys. Rev. C **65**, 061301(R) (2002).
[31] M. Honma *et al*., in Proceedings of Fourth International Conference on Exotic Nuclei and Atomic Masses (ENAM04), Eur. Phys. J. A **25**, 499 (2005).
[32] M. Horoi, B. A. Brown, and V. Zelevinsky, Phys. Rev. C **67**, 034303 (2003).
[33] B. A. Brown, A. Etchegoyen, and W. D. M. Rae, The computer code OXBASH, MSU-NSCL Report No. 524, 1998 (unpublished).
[34] C. N. Davids *et al*., Phys. Rev. C **17**, 1815 (1978).
[35] G. Audi *et al*., Nucl. Phys. **A279**, 3 (2003).
[36] A. E. L. Dieperink and T. de Forest, Phys. Rev. C **10**, 543 (1974).
[37] B. A. Brown, A. Csoto, and R. Sherr, Nucl. Phys. **A597**, 66 (1996).
[38] J. A. Tostevin, Nucl. Phys. **A682**, 320c (2001).
[39] C. A. Bertulani and P. G. Hansen, Phys. Rev. C **70**, 034609 (2004).
[40] J. Enders *et al*., Phys. Rev. C **65**, 034318 (2002).
[41] A. Gade *et al*., Phys. Rev. C **69**, 034311 (2004).
[42] A. Gade *et al*., Phys. Rev. C **71**, 051301(R) (2005).